

Superconducting properties of fractal Nb/Cu multilayers

A. Sidorenko,* C. Sürgers, T. Trappmann, and H. v. Löhneysen
Physikalisches Institut, Universität Karlsruhe, D-76128 Karlsruhe, Germany
 (Received 11 October 1995)

Multilayers of Nb and Cu with a fractal or periodic stacking sequence were prepared by electron-beam evaporation onto sapphire substrates. Their superconductivity was investigated by measurements of T_c and the temperature and angular dependence of the upper critical field B_{c2} . For low temperatures $T \ll T_c$, all samples show the characteristic behavior of two-dimensional superconductivity independent of the stacking sequence, whereas for temperatures near T_c the type of layering determines the effective dimensionality, resulting in a ‘‘multicrossover’’ behavior in fractal samples.

I. INTRODUCTION

The possibility of new mechanisms of superconductivity in layered materials¹ and the recent advances in deposition techniques have led to the intensive study of artificial modulated structures.² In addition, these investigations were motivated by the search for superconducting systems with a higher transition temperature T_c and new superconductive phenomena. These studies have become particularly important after high- T_c superconductivity was discovered in layered metal-oxide compounds. Experimental studies on artificial superconducting multilayers (SM) have mainly focused on the dependence of T_c on the modulation period Λ of the SM,^{3–6,8} on the effects of dimensionality, e.g., the so-called dimensional crossover,⁹ and on vortex motion and vortex dynamics.¹⁰

The possibility of using artificial SM for obtaining new superconducting materials was illustrated by PbTe/PbS multilayers⁵ with a critical temperature $T_c = 5.5$ K, which were composed of individually nonsuperconducting layers of the semiconductors PbTe and PbS (with an electron concentration of $\sim 10^{19}$ cm⁻³). Another example for dimensional effects in SM is the oscillatory dependence of T_c on the thickness of the superconducting layer and of a number of kinetic characteristics on the compositional modulation period Λ in Mo/Si multilayers.⁶

SM can be composed of either superconductor–insulator (or semiconductor) layers which are coupled by the Josephson effect (S/I type), or superconductor–normal-metal layers coupled by the proximity effect (S/N type). Of course, a superconductor with a much lower T_c can play the role of the normal metal in the S/N type SM.

Because of the strong temperature dependence of the superconducting Ginzburg-Landau coherence length $\xi(T) = \xi(0)/\sqrt{1 - T/T_c}$, a dimensional crossover can occur as a function of temperature T . Near T_c the perpendicular coherence length ξ_{\perp} is large, $\xi_{\perp}(T) \gg \Lambda$, and superconductivity extends over many layers. In this region a three-dimensional (3D) anisotropic behavior with a linear temperature dependence of the parallel critical field is observed:⁷

$$B_{c2\parallel}(T) = \phi_0 / 2\pi \xi_{\parallel}(T) \xi_{\perp}(T) \sim (1 - T/T_c). \quad (1)$$

Below a crossover temperature $T_{cr} < T_c$ where $\xi_{\perp}(T)$ becomes comparable to the SM period Λ , the behavior becomes two-dimensional (2D) with⁷

$$B_{c2\parallel}(T) = \phi_0 / \sqrt{2} \pi \Lambda \xi_{\parallel}(T) \sim (1 - T/T_c)^{1/2}. \quad (2)$$

Such a dimensional crossover has been observed in the temperature dependence $B_{c2\parallel}(T)$ and in the angular dependence $B_{c2}(\theta)$ in both types of SM, i.e., in the S/I type [Mo/Si,⁶ Nb/Ge,¹¹ Pb/C (Ref. 12)] and S/N type [Nb/Cu,¹³ V/Cu,¹⁴ Nb/Ta (Ref. 15)].

At temperatures $T > T_c$ the dimensional crossover can also be observed in the T dependence of the fluctuation conductivity $\sigma'(T)$. A change from 3D- to 2D-like behavior of $\sigma'(T)$ with increasing T has been measured in Nb/Si (Ref. 16) and V/Cu.¹⁷ The dimensional crossover was also observed in the fluctuation conductivity $\sigma'(T)$ of YBa₂Cu₃O_x single crystals¹⁸ and in the $B_{c2\parallel}(T)$ and $B_{c2\parallel}(\theta)$ dependences of Bi₂Sr₂CaCu₂O_x single crystals.¹⁹

In a simple periodic SM there is only one characteristic geometric length scale, the modulation period Λ . However, it is possible to prepare multilayers with several different geometric length scales, i.e., one-dimensional quasiperiodic structures²⁰ and self-similar or fractal geometries.²¹ In these systems the temperature-dependent ratio of ξ_{\perp} to the different geometric length scales may lead to new physical phenomena. The motivation to study such geometries stems in part from the numerous examples of fractal structures that exist in nature, and also because of their relation to inhomogeneous materials—percolative thin films, ceramics, and networks. A particularly nice example are two-dimensional superconducting fractal networks like Sierpinski gaskets, where the fractal structure is directly reflected in the (B, T) phase-transition line.²²

In this paper we present the results of our investigation of the superconducting properties of Nb/Cu multilayers with a fractal stacking sequence, in particular the behavior of T_c and B_{c2} , extending the previous work on fractal Nb/Cu multilayers, where a preliminary report of some B_{c2} data was already given.²³ However, for practical reasons one is limited to only a few self-similar length scales. Nevertheless, fractal features can be clearly identified.

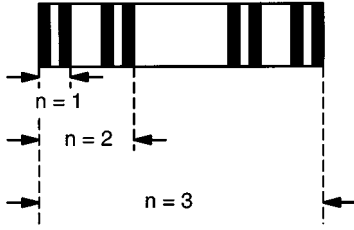


FIG. 1. Geometric structure of fractal superconducting multilayers (SM) S_n with $D_f=0.63$. Dark areas indicate the superconducting, light areas the normal conducting layers. n is the number of repeat scales.

II. SAMPLE PREPARATION AND CHARACTERIZATION

The Nb/Cu multilayers were prepared in an ultrahigh vacuum system (base pressure $< 10^{-10}$ mbar). Two electron beam sources were used for evaporating Nb (99.99% purity, Metallwerk Plansee, Reutte, Austria) and Cu (99.999% purity, Johnson Matthey) onto sapphire (1120) substrates with evaporation rates $R_{\text{Nb}}=0.4 \text{ \AA/s}$ and $R_{\text{Cu}}=1 \text{ \AA/s}$. Film thickness and evaporation rate were controlled by quartz-crystal oscillators. The deposition region was surrounded by a liquid-nitrogen-cooled shroud. Thus, the pressure could be kept below 5×10^{-10} mbar during evaporation. Further details of the system have been described elsewhere.²⁴ The substrates were outgassed at $700 \text{ }^\circ\text{C}$ for 10 min and sputtered by a 1-keV Ar^+ beam for 5 min to clean the surface from carbon contaminations. They were heated to temperatures of $\approx 1000 \text{ }^\circ\text{C}$ to allow recrystallization of the ion-bombarded sapphire surface. This procedure yields a clean and well-ordered surface as checked with *in situ* reflection high-energy electron diffraction and Auger electron spectroscopy. The deposition temperature was $30\text{--}40 \text{ }^\circ\text{C}$ to avoid mutual interdiffusion between the layers.

The geometry of the prepared fractal multilayers is sketched in Fig. 1. For a given set of fractal SM we have chosen to keep the thickness of the superconducting layers constant ($d_{\text{Nb}}=d=\text{const}$) and to vary the normal-metal thickness according to the triadic Cantor set.²⁵ Taking the dividing factor r to be $1/3$ we obtained structures with the fractal dimension $D_f=\ln 2/\ln(1/r)=0.63$ between the two limits $D_f=0$ (single superconducting film, $r=0$) and $D_f=1$ (periodic SM, $r=0.5$). The total thickness d_{tot} of a fractal multilayer S_n with a number of repeat scales n is given by $d_{\text{tot}}(S_n)=(1/r)^{n-1} \cdot (d/r)$. In addition, we prepared periodic SM with n bilayers of Nb/Cu capped with an additional Nb layer. Therefore, P_n denotes periodic SM which actually have $(n + 1/2)$ periods.

The measurements were performed in a ^4He cryostat equipped with a superconducting solenoid providing fields up to 5 T. The temperature was measured with a carbon-glass thermometer which was calibrated against a Ge thermometer in zero field. T was controlled in the range of $1.5\text{--}10 \text{ K}$ with an accuracy of $\pm 1 \text{ mK}$. The small magnetoresistance of the carbon-glass thermometer corresponds to a maximum deviation of 10 mK at 5 T compared to the temperature in zero field. The resistivity measurements were performed with an ac bridge using the conventional four-probe method. The critical temperature T_c and the upper

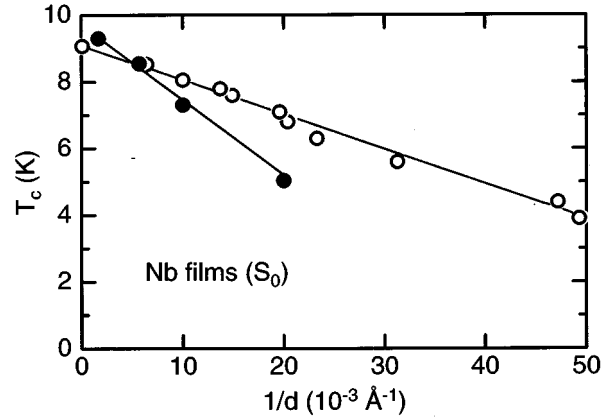


FIG. 2. T_c of single Nb films as a function of inverse film thickness: Open circles—films capped with a Si layer (Ref. 26). Solid circles—this work, where d is the “true” Nb thickness without a $20\text{-}\text{\AA}$ thick Nb oxide layer. Solid lines are guides to the eye.

critical magnetic field B_{c2} were defined as the midpoints of the resistive transitions $R(T)$ and $R(B)$.

III. RESULTS AND DISCUSSION

A. Transition temperature T_c

Before presenting data for SM, it is instructive to look at the T_c depression of Nb single films (S_0) with decreasing thickness as shown in Fig. 2, together with data from Park and Geballe.²⁶ The latter films were covered with a thin Si layer. In contrast, the presence of a nonsuperconducting oxide layer of about 20 \AA as determined from x-ray reflectivity measurements has to be taken into account in our films.²⁷ This oxide layer unavoidably builds up in ambient air during the transfer of the samples from the UHV chamber to the cryostat. Hence, the thinnest Nb single films and SM were capped with an additional $20\text{-}\text{\AA}$ Nb layer to compensate for the reduction of the superconducting layer thickness due to the oxidation. In Fig. 2 we plot T_c versus the presumably “true” Nb thickness without the oxide layer. Both data series show an almost linear T_c depression with increasing $1/d$, which is stronger for the present samples, especially at small d . The depression was explained earlier by three main mechanisms including proximity, localization, and lifetime broadening effects.²⁸ The latter seems to be important in our samples, since the residual resistivity $\rho_{10}=\rho(10 \text{ K})$ changes drastically for $d \leq 100 \text{ \AA}$, i.e., faster than d^{-1} , presumably due to an enhanced grain-boundary scattering for small d (Table I). For these films we also observe a stronger T_c depression compared to the Si-capped samples of Ref. 26, which is possibly due to the proximity effect caused by the nonsuperconducting but metallic oxide layer. The difference between both data sets increases linearly with increasing $1/d$. This is in good agreement with the proximity-effect theory in the thin-film or Cooper limit, where both thicknesses are much smaller than the coherence length.²⁹ In this case, the usual exponential decrease of T_c as a function of inverse film thickness can be approximated by a linear decrease if the normal film is sufficiently thin.

In the following we discuss the data of SM. Table I gives an overview over the properties of all investigated samples.

TABLE I. Properties of investigated samples (see text for symbols).

Nb d (Å)	Sample	D_f	d_{tot} (Å)	T_c (K)	$\xi_{\parallel}(0)$ (Å)	ρ_{10} ($\mu\Omega$ cm)	R_{300}/R_{10}
35 ^a	S_1	0.63	105	4.65	121	24.3	1.30
	S_2	0.63	315	3.07	283	6.13	1.85
	S_3	0.63	945	2.31	530	1.86	3.10
50 ^a	S_0	0	50	4.98	79	61.7	1.34
	S_1	0.63	150	5.04	131	15.2	1.42
	S_2	0.63	450	3.80	220	5.01	1.78
	S_3	0.63	1350	3.30	311	1.46	3.58
	P_3	1	350	4.07	161	18.1	1.34
	P_7	1	750	4.27	183	12.3	1.44
	100 ^a	S_0	0	100	7.31	82	34.9
S_1		0.63	300	6.64	120	7.17	2.21
S_2		0.63	900	5.66	160	2.24	2.72
S_3		0.63	2700	5.68	166	1.09	4.55
P_3		1	700	6.15	148	6.2	1.75
P_{13}		1	2700	6.26	158	5.7	1.78
175		S_0	0	175	8.75	108	6.35
	S_1	0.63	525	7.61	135	3.66	2.86
	S_2	0.63	1575	6.89	133	1.54	3.66
	S_3	0.63	4625	6.85	138	0.68	5.50
	P_4	1	1575	7.67	133	5.03	1.91
	P_6	1	2275	7.64	134	4.99	1.95
	600	S_0	0	600	9.34	131	1.70
S_1		0.63	1800	8.89	118	0.92	6.45
S_2		0.63	5400	8.79	119	0.44	7.57

^aThe single film S_0 and the outermost layer of SM had an additional 20-Å Nb layer (see text).

For periodic SM the T_c depression with decreasing d is in good agreement with an earlier study on Nb/Cu multilayers for which the deGennes-Werthamer theory of the proximity effect was applied,³ using T_c of the individual Nb layers as an adjustable parameter. There, it was shown that T_c of Nb changes for $d < 300$ Å in agreement with the $T_c(d)$ dependence of single Nb films.

Figure 3 shows the resistive superconducting transitions for three sets of fractal SM (f -SM), all with a fractal dimension $D_f = 0.63$, only differing in the thickness d of the Nb

layers. One observes three types of T_c behavior for f -SM: (1) For large $d = 600$ Å (curves ‘‘A’’) $T_c(S_1) \approx T_c(S_2)$, suggesting that T_c does not depend strongly on the fractal scale number n ; (2) for intermediate thicknesses $d = 175$ Å (curves ‘‘B’’) and $d = 100$ Å (not shown in Fig. 3), T_c decreases between S_1 and S_2 and remains constant for $n > 1$, $T_c(S_1) > T_c(S_2) = T_c(S_3)$; (3) finally, f -SM with very thin Nb layers ($d = 50$ Å, curves ‘‘C’’ in Fig. 3) show a strong depression of T_c with increasing n : $T_c(S_1) > T_c(S_2) > T_c(S_3)$.

Obviously, the type of layering and not the outer layers of our f -SM (which always have Nb as outermost layers) determine their T_c behavior. This fact is documented by the data of Table I, where T_c 's of periodic multilayers (p -SM) with different d are shown. For a given thickness d of the Nb layers, T_c of p -SM is higher than T_c of f -SM (with $n > 1$) with the same total thickness d_{tot} or the same number of layers. In addition, for ‘‘fractals’’ S_1 , T_c is always higher than or equal to T_c of p -SM with the same Nb thickness.

Figure 4 shows T_c vs $1/d$ for different f -SM, as well as for p -SM. In all cases the main effect is the decrease of T_c with decreasing d , as expected. However, the different behavior of the fractal SM described above is clearly visible. In particular, T_c decreases with increasing n for f -SM with small d , while for p -SM it stays constant or even increases slightly with increasing number of modulation periods (see Table I).

The transition temperature of multilayers with a fractal stacking sequence has been calculated by Yuan and

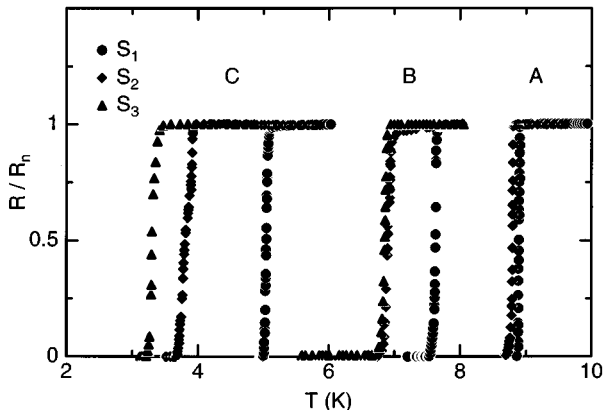


FIG. 3. Resistive transitions of three series of Nb/Cu fractal SM normalized to $R_n = R(10 \text{ K})$. Curves A: $d = 600$ Å, B: $d = 175$ Å, C: $d = 50$ Å.

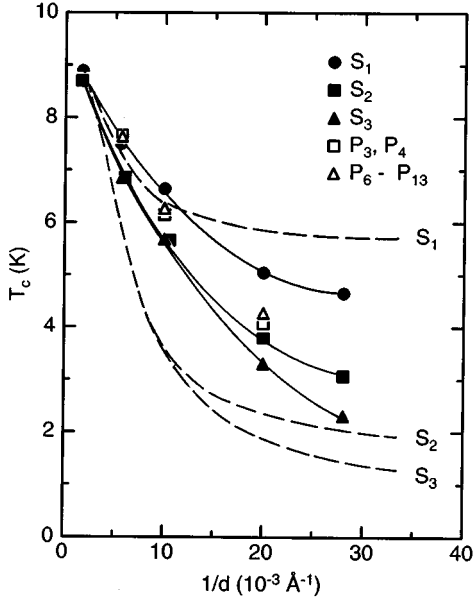


FIG. 4. T_c of Nb/Cu fractal and periodic SM vs inverse Nb thickness $1/d$. Solid lines are guides to the eye. Dashed curves show the theoretical calculation (Ref. 30) for f -SM S_1 , S_2 , S_3 with $D_f=0.63$ (see text for details).

Whitehead³⁰ in the frame of the Werthamer theory of the proximity effect. In certain limiting cases T_c of f -SM can be expressed in terms of scaling laws involving the self-similar geometry of fractal multilayers. The theory gives the reduced transition temperature $t = T/T_c^{\text{bulk}}$ as a function of the reduced thickness $\delta = kd/\xi_0$, where k is a numerical parameter and ξ_0 the BCS coherence length. We used $T_c^{\text{bulk}} = 9.38$ K (Ref. 32) and $\xi_0 = 430$ Å for bulk Nb (Ref. 31) to compare our results for f -SM with the theoretical expression for S_1 to S_3 (dashed curves in Fig. 4). k was taken to be 7.17 to yield the closest possible agreement between the theoretical curves and the experimental data for thick films ($d = 600$ Å). Although qualitative agreement between theory and experiment is observed in the sense of a progressive “ T_c splitting” with decreasing d between S_1 and f -SM with larger n described above, quantitative agreement is lacking. Theoretically, an equal diffusion constant was assumed for both normal metal and superconductor which is not the case for Cu and Nb. Furthermore, T_c of the individual superconducting layers is assumed to be independent of their thickness, the whole ensemble being subjected to a T_c depression via the proximity effect. Contributions such as weak localization and electron-electron interaction which can cause a T_c depression are not considered. However, such effects might not be important since x-ray-diffraction studies show that for layer thickness $d_{\text{Nb}}, d_{\text{Cu}} > 10$ Å the layers are very regularly stacked along the growth direction exhibiting superlattice lines around the Bragg reflections.³³ Another possible contribution to the T_c depression which is not considered in this paper, could be due to strains introduced by differences in the thermal-expansion coefficients between Nb, Cu, and the substrate.

B. Critical magnetic fields

Figure 5 shows the temperature dependence of the upper critical fields $B_{c2\parallel}$ and $B_{c2\perp}$ for three different samples: a

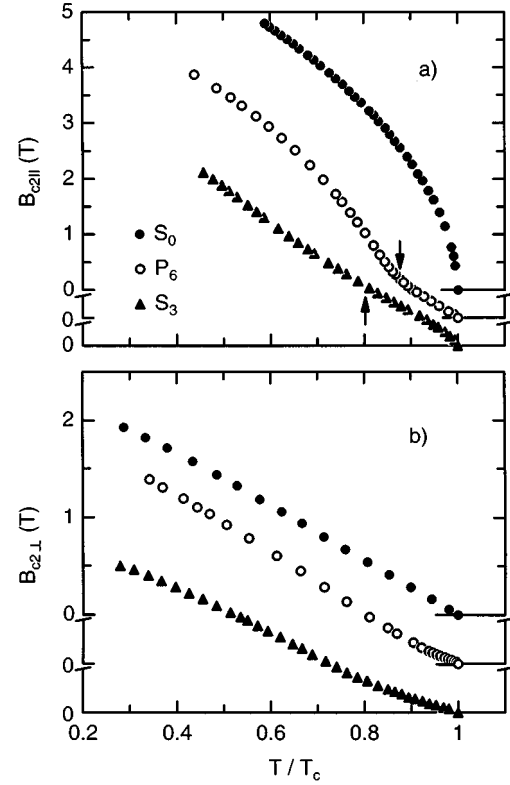


FIG. 5. Parallel critical magnetic field $B_{c2\parallel}(T)$ (a) and perpendicular critical magnetic field $B_{c2\perp}(T)$ (b) vs reduced temperature T/T_c for a single Nb film (solid circles), a periodic SM P_6 (open circles) and a fractal SM S_3 with $D_f=0.63$ (solid triangles) with $d = 175$ Å. The crossover temperatures T_{cr} are marked by arrows. Each curve is shifted upward by 0.5 T for clarity.

thin Nb film ($D_f=0$), a p -SM ($D_f=1$) and an f -SM ($D_f=0.63$). At low T all samples show 2D behavior of $B_{c2\parallel}$ [Eq. (2)] and are characterized by an effective thickness $d_{\text{eff}} = \sqrt{12}\phi_0/2\pi B_{c2\parallel}\xi_{\parallel} \approx 200$ Å which is close to the thickness of the Nb layers ($d = 175$ Å) for these samples. The single film clearly exhibits the 2D square-root behavior of $B_{c2\parallel}(T)$ at all temperatures $T < T_c$, whereas the T dependence of $B_{c2\parallel}(T)$ for f -SM and p -SM distinctly changes above a crossover temperature T_{cr} (marked by arrows). In this region, $T_{\text{cr}} < T < T_c$, $B_{c2\parallel}(T)$ can be described by

$$B_{c2\parallel}(T) \sim (1 - T/T_c)^f, \quad (3)$$

where the exponent f strongly depends on the reduced sample thickness d_{tot}/ξ_0 as shown in Fig. 6(a). f was determined from a log-log plot of $B_{c2\parallel}(T)$ vs $(T_c - T)/T_c$ [Fig. 6(b)]. For $d_{\text{tot}}/\xi_0 < 2$ all samples exhibit 2D behavior, i.e., $f = 0.5$ [Eq. (3)], in the whole temperature range $T < T_c$ independent of the type of layering. In simple terms, the $B_{c2\parallel}(T)$ dependence near T_c is not affected by the different length scales if d_{tot} is smaller than ξ_0 . For samples with $d_{\text{tot}}/\xi_0 \geq 2$ the type of layering determines the exponent: For p -SM as well as for f -SM with $n < 3$ (S_1 and S_2) 3D behavior, i.e., $f = 1$, is observed, whereas fractals S_3 clearly show $f \approx 0.75$. According to the Matijasevic-Beasley scaling model,²¹ near T_c the strongly T -dependent coherence length $\xi_{\perp}(T)$ becomes successively comparable to the different

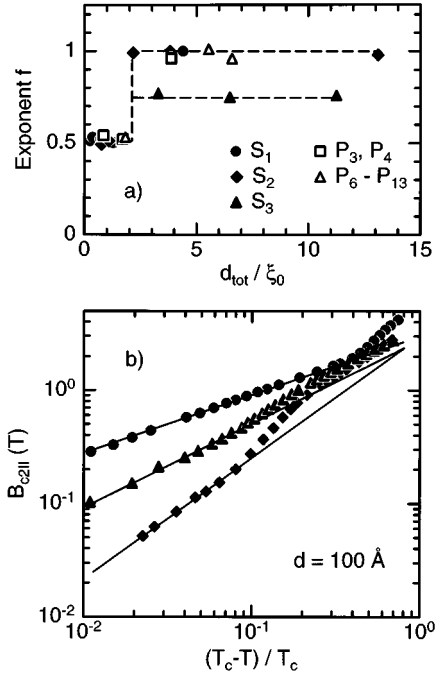


FIG. 6. (a) Exponent f vs reduced thickness d_{tot}/ξ_0 for f -SM and p -SM. Dashed lines are guides to the eye. (b) Log-log plots of $B_{c2||}$ vs reduced temperature for f -SM samples (S_1 - S_3) with $d=100 \text{ \AA}$ and $D_f=0.63$. Solid lines show the fits near T_c to obtain f according to Eq. (3).

fractal scales. This leads to the ‘‘multicrossover’’ of the parallel critical magnetic field $B_{c2||}(T)$ which should be almost 2D-like with a logarithmic correction:

$$B_{c2||}(T) = \frac{\phi_0}{2\pi\xi_{||}(T)\xi_{\perp}(T)} \sim -(1-t)^{1/2}/\ln(1-t). \quad (4)$$

This dependence arises from a self-consistency condition imposed on the transition temperature and the coherence length.²¹ Over a small temperature interval near T_c , Eq. (4) may be approximated by an algebraic T dependence [Eq. (3)]. For samples with a fractal stacking sequence an exponent $0.5 < f < 1$ is expected from the scaling model²¹ and this is observed for all samples S_3 in the temperature region $T_{\text{cr}} < T < T_c$.

Turning to $B_{c2\perp}(T)$ [Fig. 5(b)], no simple behavior in the context of the theory of Werthamer, Helfand, and Hohenberg,³⁴ and Maki³⁵ is observed for fractal and periodic SM. $B_{c2\perp}(T)$ shows the expected linear behavior near T_c , but for temperatures $T < 0.8T_c$ a positive curvature is clearly seen. However, this has nothing to do with the fractal stacking sequence and has also been found in previous studies of periodic SM including Nb/Cu and Nb/Ta multilayers.^{13,15} The origin of this curvature in the temperature dependence of $B_{c2\perp}$ is still unclear. In order to extract an estimate for the Ginzburg-Landau coherence length we calculated $\xi_{||}(0)$ from the slope of $B_{c2\perp}(T)$ at T_c ,

$$\xi_{||}(0) = [-dB_{c2\perp}(T)/dT|_{T_c} 2\pi T_c / \phi_0]^{-1/2}$$

(Table I).

For a few multilayers, the complete angular dependence of the upper critical field was studied. The multicrossover

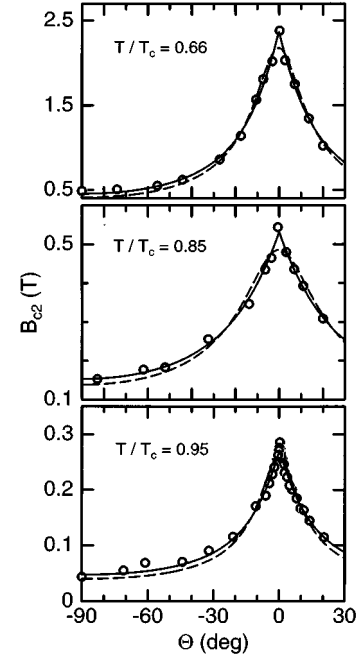


FIG. 7. Angular dependence of the critical magnetic field $B_{c2}(\theta)$ at different T/T_c for f -SM S_3 with $d=175 \text{ \AA}$ and $D_f=0.63$. Solid curves are fits using the Tinkham formula [Eq. (5)], dashed lines show fits using the Lawrence-Doniach theory [Eq. (6)].

behavior of our f -SM can nicely be observed in the angular dependence $B_{c2}(\theta)$, where θ is the angle between the film plane and the applied magnetic field. Figure 7 shows $B_{c2}(\theta)$ for S_3 ($D_f=0.63$) at different reduced temperatures T/T_c . Obviously, at all temperatures $B_{c2}(\theta)$ follows the Tinkham equation for a 2D superconductor³⁶ with a cusp at an orientation parallel to the magnetic field ($\theta=0$):

$$\left| \frac{B_{c2}(\theta)\sin(\theta)}{B_{c2\perp}} \right| + \left(\frac{B_{c2}(\theta)\cos(\theta)}{B_{c2||}} \right)^2 = 1. \quad (5)$$

The Lawrence-Doniach approximation for a 3D anisotropic superconductor³⁷

$$B_{c2}(\theta) = \frac{\phi_0}{2\pi\xi_{||}^2(T)[\sin^2\theta + (B_{c1}/B_{c||})^2\cos^2\theta]^{1/2}} \quad (6)$$

is not compatible with the data. The difference between the two types of behavior is seen particularly well near $\theta=0$. In summary, we find that at low temperatures ($T < T_{\text{cr}}$) the 2D behavior of fractals is governed by the dimension of the Nb layers, while for $T_{\text{cr}} < T < T_c$ the curvature of $B_{c2||}(T)$ and the 2D behavior of $B_{c2}(\theta)$ reflect the multicrossover regime as a result of the existence of a series of length scales in the structure. Literally speaking, at any given temperature the f -SM ‘‘offers’’ a layer arrangement with the ‘‘correct’’ effective thickness to match the respective coherence length $\xi_{\perp}(T)$.

IV. CONCLUSION

S/N multilayers consisting of alternating Nb and Cu layers with a fractal stacking sequence and a fractal dimension $D_f=0.63$, and also with the two limiting cases $D_f=0$ (thin

superconducting film) and $D_f=1$ (periodic SM) were prepared. The samples show a dependence of the transition temperature T_c on Nb thickness and number of repeat scales in qualitative agreement with the proximity-effect theory developed for multilayered superconductors with a self-similar structure.³⁰ The behavior of the parallel upper critical magnetic field is directly related to the type of layering.

At low temperatures ($T \ll T_c$) all samples exhibit the same 2D behavior essentially governed by the topological dimension of the individual superconducting elements (i.e., 2D), independent of the fractal dimensionality D_f of the samples. The layering geometry is, however, important in the temperature region $T_{cr} < T < T_c$ and determines the dimension of the samples near T_c , i.e., 2D for thin films, 3D for periodic SM, and quasi-2D [Eq. (3)] for fractal SM with $n > 2$.

The angular dependence of the upper critical magnetic field $B_{c2}(\theta)$ of fractal SM corresponds to the Tinkham theory for a 2D superconductor at all temperatures, reflecting

the multicrossover behavior in fractal SM, as long as the T -dependent coherence length is comparable to a certain scale of fractal.

One might speculate that the existence of a number of such scales in some other systems, such as quasiperiodic,³⁸ random² and textured films³⁹ might be the reason for the anomalous curvature in the critical field $B_{c2\parallel}(T)$ near T_c often observed in these systems. Hence, artificial SM with fractal geometry are a suitable model object for either theoretical simulations or experimental studies of the real disordered superconducting systems.

ACKNOWLEDGMENTS

We would like to thank V. Matijasevic, J. Aarts, A. Varlamov, B. J. Yuan, and L. Glazman for helpful discussions. One of us (A.S.) is grateful to the Alexander von Humboldt Foundation for financial support.

*Permanent address: Institute of Applied Physics, Kishinev, 277028 Moldova.

¹V. L. Ginzburg, in *High Temperature Superconductivity*, edited by V. L. Ginzburg and D. A. Kirzhnits (Consultants Bureau, New York, 1982).

²V. Matijasevic and M. R. Beasley, in *Metallic Superlattices*, edited by T. Shinjo and T. Takada (Elsevier, Amsterdam, 1987).

³I. Banerjee, Q. S. Yang, C. M. Falco, and I. K. Schuller, *Solid State Commun.* **41**, 805 (1982).

⁴M. G. Karkut, D. Ariosa, J. M. Triscone, and Ø. Fischer, *Phys. Rev. B* **32**, 4800 (1985).

⁵I. M. Dmitrenko, N. Ya. Fogel, and V. G. Cherkasova, *Fiz. Nizk. Temp.* **19**, 747 (1993) [*Low Temp. Phys.* **19**, 533 (1993)].

⁶E. I. Bukhstab, V. Yu. Kashirin, N. Ya. Fogel, V. G. Cherkasova, V. V. Kondratenko, A. I. Fedorenko, and S. A. Yulin, *Fiz. Nizk. Temp.* **19**, 704 (1993) [*Low Temp. Phys.* **19**, 506 (1993)].

⁷S. T. Ruggiero and M. R. Beasley, in *Synthetic Modulated Structures*, edited by L. L. Chang and B. C. Giessen (Academic, New York, 1985).

⁸E. Majkova, S. Luby, M. Jergel, H. v. Löhneysen, C. Strunk, and B. George, *Phys. Status Solidi A* **145**, 509 (1994).

⁹B. Y. Jin and J. B. Ketterson, *Adv. Phys.* **38**, 189 (1989).

¹⁰W. R. White, A. Kapitulnik, and M. R. Beasley, *Phys. Rev. Lett.* **66**, 2826 (1991).

¹¹S. T. Ruggiero, T. W. Barbee, and M. R. Beasley, *Phys. Rev. Lett.* **45**, 1299 (1980).

¹²J. P. Locquet, D. Neerink, and H. van der Straaten, *Jpn. J. Appl. Phys.* **26**, 1431 (1987).

¹³C. S. L. Chun, G. G. Zheng, J. L. Vincent, and I. K. Schuller, *Phys. Rev. B* **29**, 4915 (1984).

¹⁴A. S. Sidorenko, V. I. Dediu, and A. G. Sandler, *Bull. Mater. Sci.* **14**, 895 (1991); V. I. Dediu, V. V. Kabanov, and A. S. Sidorenko, *Phys. Rev. B* **49**, 4027 (1994).

¹⁵P. R. Broussard and T. H. Geballe, *Phys. Rev. B* **35**, 1664 (1987).

¹⁶H. Obara, K. Uchinokura, and S. Tanaka, *Physica C* **157**, 37 (1989).

¹⁷V. I. Dediu, V. V. Kabanov, A. G. Sandler, and A. S. Sidorenko, *Phys. Lett. A* **157**, 488 (1991).

¹⁸A. Kapitulnik, *Physica C* **153-155**, 520 (1988).

¹⁹R. Fastampa, M. Giura, P. Marcon, and E. Silva, *Phys. Rev. Lett.* **67**, 1795 (1991).

²⁰J. L. Cohn, J. J. Lin, F. J. Lamelas, H. He, R. Clarke, and C. Uher, *Phys. Rev. B* **38**, 2326 (1988).

²¹V. Matijasevic and M. R. Beasley, *Phys. Rev. B* **35**, 3175 (1987).

²²J. M. Gordon, A. M. Goldman, J. Maps, D. Costello, R. Tiberio, and B. Whitehead, *Phys. Rev. Lett.* **56**, 2280 (1986); O. Entin-Wohlman, A. Kapitulnik, S. Alexander, and G. Deutscher, *Phys. Rev. B* **30**, 2617 (1984).

²³A. Sidorenko, C. Sürgers, T. Trappmann, and H. v. Löhneysen, *Physica C* **235-240**, 2615 (1994). In this report data for another set of samples, labeled with $D_f=0.5$ were also communicated. However the layer sequence of this series was actually such that $D_f=0.5$ for S_1 and $D_f \approx 0.63$ for S_2 and S_3 .

²⁴C. Sürgers and H. v. Löhneysen, *Thin Solid Films* **219**, 69 (1992).

²⁵B. B. Mandelbrot, *The Fractal Geometry of Nature* (Freeman, San Francisco, 1983).

²⁶S. I. Park and T. H. Geballe, *Phys. Rev. Lett.* **57**, 901 (1986).

²⁷C. Sürgers, C. Strunk, and H. v. Löhneysen, *Thin Solid Films* **239**, 51 (1994).

²⁸S. I. Park and T. H. Geballe, *Physica B* **135**, 108 (1985).

²⁹W. Silvert and L.N. Cooper, *Phys. Rev.* **141**, 336 (1966).

³⁰B. J. Yuan and J. P. Whitehead, *Physica C* **160**, 287 (1989).

³¹D. K. Finnemore, T. F. Stromberg, and C. A. Swenson, *Phys. Rev.* **149**, 231 (1966).

³²D. Hemming, R. Sati, and J. D. Leslie, *Can. J. Phys.* **48**, 1254 (1970).

³³I. K. Schuller, *Phys. Rev. Lett.* **44**, 1597 (1980); W. P. Lowe, T. W. Barbee, T. H. Geballe, and D. B. McWhan, *Phys. Rev. B* **24**, 6193 (1981).

³⁴E. Helfand and N. R. Werthamer, *Phys. Rev.* **147**, 288 (1966); N. R. Werthamer, E. Helfand, and P. C. Hohenberg, *ibid.* **147**, 295 (1966).

³⁵K. Maki, *Physics* **1**, 21 (1964); **1**, 127 (1964).

³⁶M. Tinkham, *Phys. Rev.* **129**, 2413 (1963).

³⁷W. E. Lawrence and S. Doniach, in *Proceedings of the 12th International Conference on Low Temperature Physics*, Kyoto, 1970, edited by E. Kanda (Academic Press of Japan, Tokyo, 1971), Vol. 12, p. 361.

³⁸M. G. Karkut, J. M. Triscone, D. Ariosa, and Ø. Fischer, *Phys. Rev. B* **34**, 4390 (1986).

³⁹A. S. Sidorenko, E. V. Minenko, N. Ya. Fogel, R. I. Shekhter, and I. O. Kulik, *Phys. Status Solidi A* **52**, K89 (1979).